SERI/TP-252-3013
UC Category: 62a
DE87001123

Experiments and Analysis on the Molten-Salt Direct-Contact Absorption Receiver Concept

Mark S. Bohn
K. Y. Wang

November 1986

Prepared for the Second ASME/JSME
Thermal Engineering Conference
Honolulu, Hawaii
22-27 March 1987

Prepared under Task No. 5122.210
FTP No. 5-651

Solar Energy Research Institute
A Division of Midwest Research Institute

1617 Cole Boulevard
Golden, Colorado 80401-3393

Prepared for the
U.S. Department of Energy
Contract No. DE-AC02-83CH10093

Printed in the United States of America
Available from:
National Technical Information Service
U.S. Department of Commerce
5285 Port Royal Road
Springfield, VA 22161

Price: Microfiche A01
Printed Copy A02

Codes are used for pricing all publications. The code is determined by the number of pages in the publication. Information pertaining to the pricing codes can be found in the current issue of the following publications, which are generally available in most libraries: *Energy Research Abstracts, (ERA); Government Reports Announcements* and Index (*GRA* and I); *Scientific and Technical Abstract Reports (STAR);* and publication, NTIS-PR-360 available from NTIS at the above address.

ABSTRACT

This paper presents results of recent experiments on the Direct Absorption Receiver (DAR) concept using molten salt as the working fluid. The DAR concept may result in a solar central receiver that costs 50% less than the current tube receiver and has significatnly lower operational and maintenance costs. These experiments were aimed at determining whether the DAR concept is technically feasible and were carried out at the Advanced Components Test Facility, Atlanta, Ga. Results are based on several days of operating with solar flux ranging up to 50 W/cm^2 and also on a numerical model that is capable of predicting the thermal performance of the DAR salt film. Issues relating to thermal efficiency, absorber-to-salt heat transfer, and salt film stability are addressed.

NOMENCLATURE

C_p	specific heat
h	heat transfer coefficient
k	thermal conductivity
L	flow length
$\dot{m}$	mass flow rate
Nu	Nusselt number
Pr	Prandtl number
q	incident flux, a function of x
q_R	radiative flux
Q_{in}	integrated incident flux = $W_o\int^L q(x)\,dx$
Re	Reynolds number, Γ/μ or $4\Gamma/\mu$
T	temperature
u	velocity in x-direction
W	absorber width
x	coordinate parallel to the flow direction
y	coordinate perpendicular to the flow direction
z	dummy variable

Greek

Γ	mass flow per unit absorber width
ε	emissivity
η_t	thermal efficiency
μ	dynamic viscosity
ρ	density or reflectivity
σ	Stefan-Boltzmann constant

Subscripts

a	air
i	inlet value
o	outlet value
peak	largest value determined experimentally
s	salt

INTRODUCTION

The concept of a direct absorption receiver (DAR) is based on absorption of concentrated solar flux within a receiver working fluid without a containment surface between the working fluid and the incident solar flux. In practice, the working fluid is directly exposed to the flux by allowing the fluid to flow by gravity in a film or a curtain in an open cavity (or possibly external) receiver. In a conventional receiver, the working fluid is contained in tubes and the radiation impinging on the tube outer surface is absorbed on the tube surface and transferred to the working fluid by conduction through the tube wall.

Direct absorption has several potential advantages over a conventional receiver using tubes. First, without an intervening tube wall, there is no temperature drop, and the working fluid is at the highest temperature in the system. This reduces material problems and receiver reradiation losses and delivers a higher temperature working fluid to a process, thereby increasing its thermodynamic efficiency. Second, the receiver will cost less (possibly 50% less than the current tube receivers) and will operate more reliably because of the simpler design and reduced thermal stress/ cycling problems. Finally, the receiver can tolerate much higher flux levels since the flux is absorbed directly in the working fluid. This further decreases the cost of the receiver since it could be smaller for the same heat duty.

Potential working fluids for a DAR include molten salt and solid particles. Hruby (1) discusses a DAR that uses a falling curtain of sand to absorb the solar

flux. Hunt (2) discusses a DAR in which very small carbon particles absorb the solar flux and transfer the heat to the gas in which they are suspended. In this paper we will focus on a DAR that uses molten salt as the working fluid.

Although falling film heat exchangers are commonly used in industry, several issues related to the DAR application arise. Generally, industrial falling film heat exchangers transfer heat to the liquid film from a solid surface. For example, a common arrangement is for the liquid film to flow down the outside diameter of a vertical pipe and heat is added from the pipe wall to the film. However, in a DAR the solar flux falls on the film where it is partially reflected, partially transmitted to the solid surface containing the film (the absorber), and partially absorbed in the film. In addition, significantly higher flux levels will be used in the DAR than in falling film heat exchangers, on the order of 1 MW/m^2. Finally, the working fluid of interest, molten salts (nitrates or carbonates), exhibit property values quite different from common industrial heat transfer fluids. Most notably are the high surface tension (110 to 220 dyne/cm), low contact angles, and the large variations in viscosity caused by the wide temperature ranges under which the molten salts will be used. Issues raised by these differences are that existing models for tube-type receivers may be inadequate for predicting DAR thermal efficiency; existing heat transfer models or correlations may not be applicable to the case where flux is absorbed directly in the film and may be questionable even for the transparent film, considering the properties of the liquid and the high fluxes; and stability of the falling film under the high flux and with the unusual properties of the liquid film may not be predictable from existing correlations.

The objective of the research described in this paper is to provide analyses and supporting experimental data to predict the heat transfer characteristics, thermal efficiency, and stability of the DAR falling molten salt film. By way of background, we first briefly describe pertinent literature on direct absorption receivers; we present important details of a DAR heat transfer model; and then describe the experimental apparatus used to measure the characteristics of the DAR film. Results are presented in the form of the film thermal efficiency, absorber-to-salt heat-transfer coefficient, and the film stability. These are then discussed in light of the previously described literature and analyses. More details on this work may be found in Bohn et al. (3).

BACKGROUND

The DAR concept appears to have been discussed first by Brumleve (4) in which he points out the potential advantages of DAR, develops preliminary cost estimates for a system using DAR, and discusses some of the research needs. Brumleve (5) presented data that showed that if a dopant is added to the normally transparent salt, very high fluxes can be tolerated. For a 2-mm film thickness exposed to 6-MW/m^2 flux, the absorber temperature exceeded the salt temperature by less than 3 deg C. In this case the salt was doped with 0.1% by weight cobalt oxide suspension.

Wang and Copeland (6) and Webb and Viskanta (7) developed a model for the heat transfer to study the mechanisms in a falling liquid film exposed to incident flux. The model allows one to study the temperature of the substrate, distribution of temperature in the salt film, and the effect of dopants used to darken the salt. The issue of salt film stability was treated by Wang et al. (8) and by Newell et al. (9). They discuss film stability at very low flow rates and high flow rates, formation of dry patches due to the thermocapillary effect, film thickness, and interaction with air flow.

HEAT TRANSFER ANALYSIS

The model presented here analyzes the heat transfer through a falling liquid film with incoming radiation as the energy input. As illustrated in Fig. 1, the film is exposed to incident flux q(x) split into two bands at 2 μm. The flux below the cutoff wavelength is considered as coming from the concentrated solar flux, and the flux above the cutoff represents the radiation from internal surfaces of the receiver cavity. Measurements during the experimental program described here indicate that the fluxes represent about 88% and 12%, respectively, of the total energy input.

The flux incident on the salt film is partially reflected at the salt and air interface; the remainder passes through the film and is partially absorbed in the film. The amount of absorption in the film depends on the optical absorption coefficient of the salt film. The fraction not absorbed is incident on the absorber surface where it is partially absorbed and re-emitted, and partially reflected, depending on the specified radiative property of the absorber surface. A two-dimensional energy equation for the liquid film is used to solve for the temperature distribution in the film.

Flow conditions such as velocity and film thickness are determined from the momentum equation. We define the film Reynolds number as

$$\mathrm{Re} = \Gamma/\mu \ , \qquad (1)$$

where Γ is the mass flow rate per unit width and μ is the fluid viscosity. (The Reynolds number, $\mathrm{Re} = 4\Gamma/\mu$, is also used in the literature.)

Various studies have been directed in the area of hydrodynamics (10) and convective heat transfer (11,12) of thin falling film flow. The studies usually suggest that laminar flow may be maintained for Re below 400, though this criteria may change because of different conditions, such as surface roughness, flow inlet conditions, or initial perturbations. A recent work by Takahama and Kato (13) suggests that the transition Re also depends on the longitudinal distance from the leading edge of the flow channel, and they report a transition Reynolds number (Γ/μ) ranging from 400 to 800 based on results from water experiments.

Although surface waves exist for Re larger than 5, Hirshburg and Florschuetz (14) indicate that the Nusselt equation, described below, still provides a good prediction for the average film-thickness/flow-rate correlation. Thus, a constant film thickness is used in the present heat transfer analysis. Careful observation during our experiments did not reveal any waviness or turbulent flow for Reynolds numbers (Γ/μ) as high as 1300. Hence, we will use laminar flow analysis here. The present heat transfer model can be extended to handle turbulent flow problems by adding an eddy diffusivity term in the energy equation, as described by Seban (11).

For a steady-state laminar falling film, the energy equation is

$$\rho C_p u \frac{\partial T}{\partial x} = \frac{\partial}{\partial y}\left(k \frac{\partial T}{\partial y}\right) - \frac{\partial q_R}{\partial y} \ , \qquad (2)$$

where x and y are the directions parallel and perpendicular to the flow, respectively. Other properties are defined in the nomenclature. In the equation, the quantity $-\partial q_R/\partial y$ is the radiative energy gain, which is

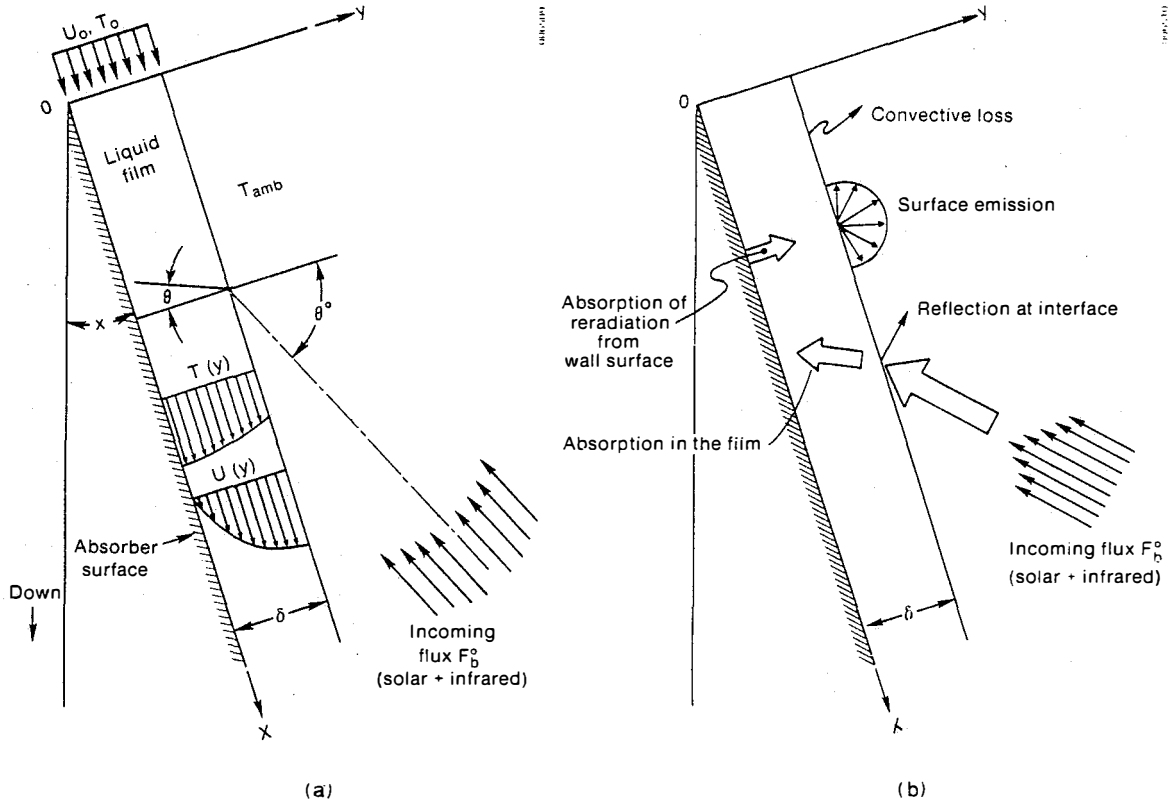

Fig. 1. Nomenclature for the Heat Transfer Model

caused by radiative absorption in the salt film from the incident radiation and from the reflected and re-emitted radiation from the absorber surface. Details of the analysis may be found in Wang and Copeland (6).

The experimentally determined flux distribution on the absorber can be approximated as a three-segment linear curve fit:

$$\begin{aligned} q(x)/q_{peak} &= 0.51 + 0.47x/L \quad \text{for } 0 \le x/L < 0.47 \\ q(x)/q_{peak} &= 0.73 + 0.87(x/L - 0.47) \quad \text{for } 0.47 \le x/L < 0.78 \\ q(x)/q_{peak} &= 1 \quad \text{for } 0.78 \le x/L < 1. \end{aligned} \tag{3}$$

The measurements also showed that the horizontal flux variation across the absorber is less than 8%, thus, justifying the two-dimensional model.

The boundary conditions for equation (2) are the same as those given in Wang and Copeland (6). At the air-salt interface, an energy gain is caused by radiative absorption and energy loss by radiative re-emission and convection. Little information is available on the heat transfer coefficent h from existing literature. In this work we used the value obtained from flow over a flat plate with the same velocity as the salt film as a guideline. Our calculations indicate that a variation in h from 0.1 W/m^2 K to 50 W/m^2 K has a very small effect on the temperature rise across the film because radiation absorption dominates the heat transfer mechanism at the interface. Thus, a precise estimate of h is unnecessary. The energy equation is solved by an implicit finite difference method. From the solution we may calculate the heat transfer at the absorber/salt interface and the thermal efficiency of the film.

The numerical model previously described calculates losses from the salt film; however, it is useful to consider a model based on simple physical principles that can also predict the thermal efficiency of the film. We assume that the absorbing surface is adiabatic, so the only losses are from the air/salt interface. These consist of incident radiation reflected from the interface, reradiation losses from the film and convective losses to the air in the cavity. Generally, the convective loss is much smaller than the other two losses. Hence, thermal efficiency can be expressed as:

$$\eta_t = 1 - \rho_s - \frac{\varepsilon_s \sigma \overline{T}_s^4}{(Q_{in}/W)}, \tag{4}$$

which allows us to calculate film efficiency as a function of average salt film temperature and incident flux.

FILM STABILITY

Stability of the salt film in a DAR is of concern because if the film suddenly ceases to wet the absorber surface, damage is almost certain to result. Research on the stability of falling films has been ongoing for years, especially in the isothermal case. This case is mostly of academic interest for the DAR as it only describes how and when the film breaks down at very low flow rates in the absence of solar flux. Under such

conditions a minimum flow is reached, below which the film breaks into several rivulets. For further discussions on this aspect of film breakdown, see Hartley and Murgatroyd (15).

More important to the DAR is film breakdown due to the presence of flux. The mechanism here is the thermocapillary effect. Since the surface tension of the molten salt decreases with increasing temperature, fluid near a local hot spot will tend to move away from the hot spot. The hot spot may originate as a result of nonuniform flux or local nonuniform film thickness, either of which are certain to occur in a DAR film flow. As the fluid moves away from the hot spot, the film thins, causing greater overheating. Eventually, a dry spot can form. Simon and Hsu (16) present a simplified model of this phenomenon and data that support the model. However, the model requires one experimentally-determined constant that depends on the fluid tested. Thus, application of Simon and Hsu's results to the molten salt film is tenuous. However, the phenomenon described by their paper is probably applicable to DAR and suggests that flux nonuniformities or film waviness could lead to film breakdown.

EXPERIMENT

The experimental effort described in this report was designed to provide data that could be compared with the heat transfer model discussed previously and that describe the stability of the salt film at low flow rates and at high flow rates in the presence of a wide range of solar flux levels and to provide operational experience with the DAR under actual solar flux.

Salt Flow Apparatus

A schematic of the molten salt test loop is shown in Fig. 2. Salt is delivered to the absorber panel (see Fig. 3) by a cantilever centrifugal pump located in the salt storage tank. Nominal flow rates range from 0.26 to 2.3 m^3/h. We established the salt temperature using double-sheath Inconel trace heating elements attached to the outside of either tank; the temperature can be adjusted up to 900 deg C. After the salt drains from the absorber panel, it flows by gravity back to the tank where it can be cooled by air flow in a heat exchange coil located in the tank. All salt lines are heated with the same heat trace used on the salt tank. The entire test loop is fabricated from Inconel 600. Tank 2, shown in Fig. 2, is used to deliver very low salt flow rates, from 0.03 to 0.3 m^3/h.

Referring to Fig. 3, salt is delivered to an inlet manifold located at the top of the absorber panel. A small packed bed in the inlet manifold damps flow pulsations and delivers the salt to a chamber just upstream of the weir. The salt then flows over the weir and down the absorber panel where 0.610 m flow length

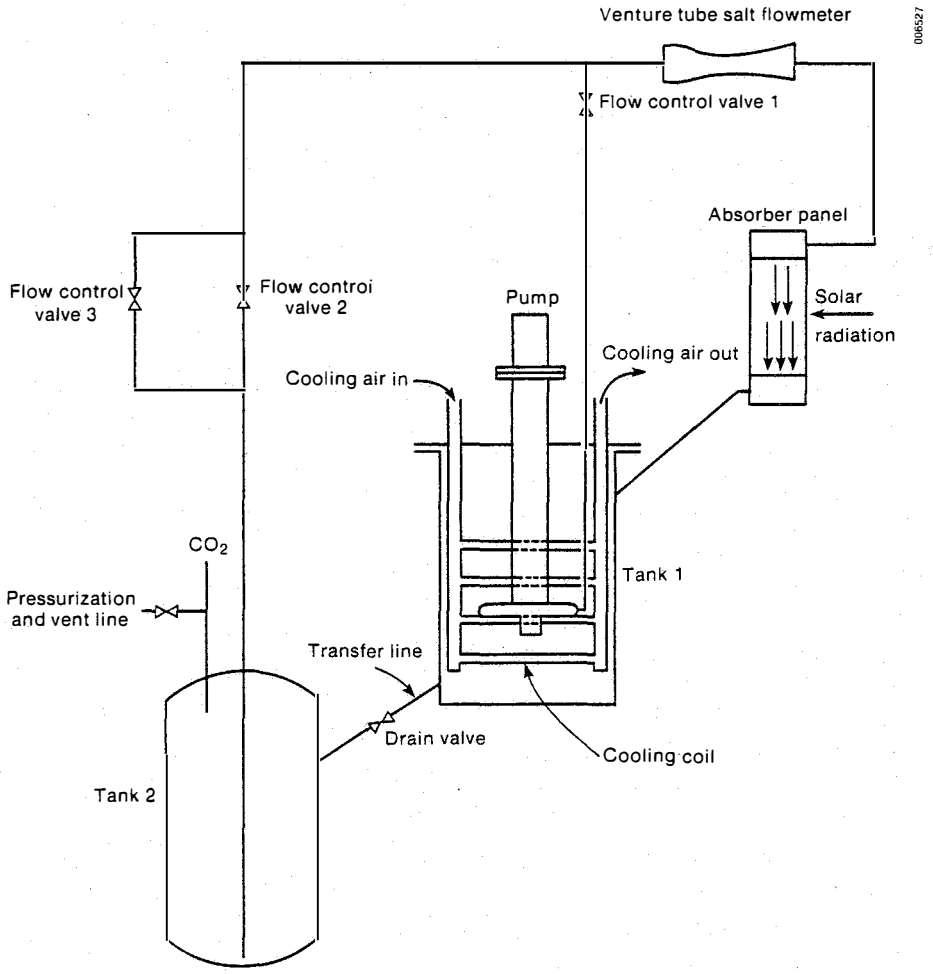

Fig. 2. Schematic of the Molten Salt Test Loop

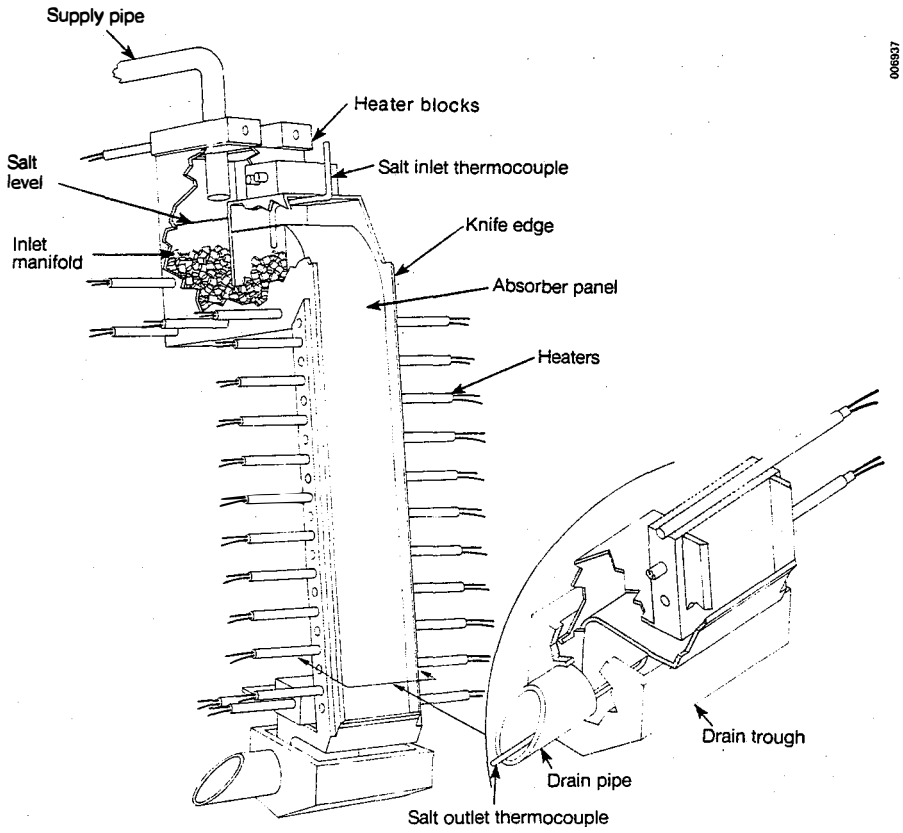

Fig. 3. Absorber Panel Assembly

and 0.150 m flow width is exposed to the solar beam. The absorber panel is tilted 5 deg from vertical.

In Fig. 4 the absorber panel is shown attached to the cavity required to redirect the vertical solar beam at the test facility onto the absorber panel. This cavity was fabricated from slip-cast fused silica with a solar-weighted reflectivity of 0.94. Because of its high reflectivity, the cavity was effective in redirecting the solar beam onto the salt film. We determined that approximately 88% of the flux incident on the salt film was in the solar spectrum. The remaining 12% was primarily infrared emitted from the cavity surface. This cavity is not typical of a commercial DAR but was required for experimental purposes.

During this test program, a commercial grade (98.5% purity) eutectic of lithium, sodium, and potassium carbonate was used as the heat transfer medium. Molar composition of the eutectic is 43.5%, 31.5%, and 25.0%, respectively, and the melting point is 397 deg C. A practical minimum working temperature is 500 deg C; we carried out tests at 500 deg, 600 deg, and 700 deg C.

Test Facility

All tests described in this paper were carried out at the Advanced Component Test Facility (ACTF) of the Georgia Tech Research Institute, Atlanta, Ga. This facility consists of 550 heliostats deployed in an octagonal array around a central experiment support tower. Data were recorded by a computer data acquisition system based on a Hewlett-Packard 1000 minicomputer.

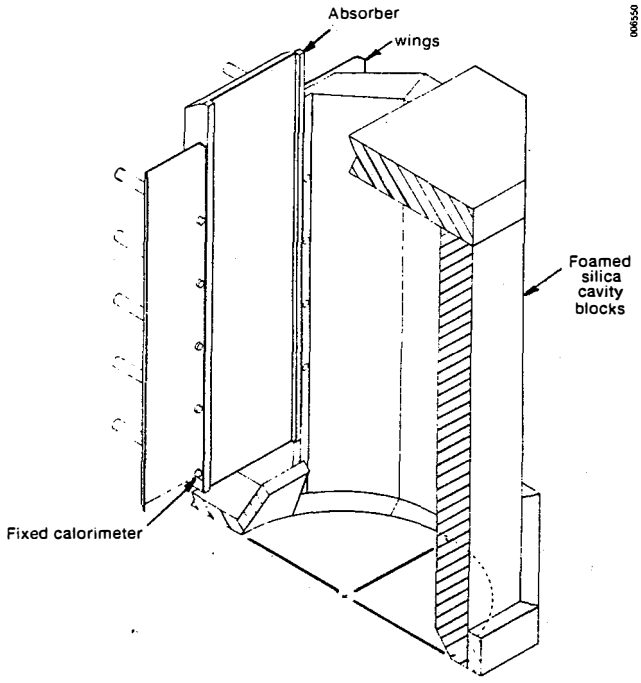

Fig. 4. Section View of Absorber Installed in Cavity

SERI

Instrumentation

Primary instrumentation involved temperature, salt flow rate, and solar flux measurements. All thermocouples were Chromel-Alumel (Type K). Salt flow rate was determined from the thickness of the salt film on the top of the absorber weir.

Flux was measured by a series of 10 fixed (see Fig. 4) and 6 movable transducers of the water-cooled Gardon gauge type. The movable transducers were attached to a water-cooled rake and were used to determine the horizontal variation of flux impinging on the absorber plate. Since this variation was found to be minimal (rms variation from the mean was 8% at solar noon and about 12% at 9 a.m. solar time), we relied on the fixed transducers to provide the flux distribution on the absorber plate for all subsequent tests [see equation (3)].

A detailed analysis of all experimental errors is presented by Bohn et al. (3). The analysis showed that the uncertainty in measured efficiency is +16.6%, -8.7%. The uncertainty in the measured dimensionless heat transfer coefficient is +14.8%, -8.4%. A bias error of +9.6% on the measured flux (caused by uncertainties in the flux transducer calibration between solar flux and infrared flux) contributes most to the experimental uncertainties.

Test Procedure

After a series of debugging tests carried out on the ground over a six week period, we raised the test loop to the top of the ACTF tower and commenced testing with solar flux. Concerns about film stability in the presence of solar flux led us to bring up the flux in stages before achieving full power for the first time. After completing this, we measured the flux distribution on the absorber plate with the movable flux rake as described previously and then began detailed testing.

During the test, the variables we adjusted included salt flow rate, inlet salt temperature, and solar flux. During clear days, we used the period near solar noon to carry out experiments with variable salt flow rate and fixed flux and the period during early morning and late afternoon to operate with fixed salt flow rate and increasing or decreasing solar flux. Three important quantities were measured: salt film thermal efficiency, heat transfer coefficient between the salt film and the absorber panel, and stability of the salt film.

The entire test loop including the absorber inlet manifold, absorber panel, and drain line were brought up to about 600 deg C with the heat tracing (these components were left at this temperature during the entire test program). The salt then began to flow, usually in the 0.2 to 2.0 m^3/h range depending on the test plan for the day. A receiver aperture shutter was closed and the beam brought up (focused on the shutters). When the heliostats stabilized and had begun tracking, the shutters were opened exposing the cavity and absorber panel to the flux. From a cold startup, approximately 30 minutes of full-flux operation was needed to establish quasi-steady conditions. By quasi-steady we mean that the absorber panel and salt temperatures had equilibrated but the cavity interior walls had not. We found that the cavity heated very slowly over a period of several hours, but this did not seem to affect flux or temperature readings, which was consistent with the fact that we measured nearly 88% of the flux in the short wavelengths.

Data were acquired at one second per complete cycle of all channels. Trend line indicators were used to help determine when steady conditions were reached. Typically, a new flow condition would be established, and if clear sky conditions prevailed, about 10 min were required before the data appeared to be steady again. New operating conditions were then established.

RESULTS AND DISCUSSION

Flow Visualization

Before discussing the quantitative measurements, it is worthwhile to first discuss our observations of salt flow down the absorber plate. These flow visualization experiments were performed during the aforementioned ground test before the cavity was assembled around the absorber plate. The primary objectives of the flow visualization experiments were to determine if the salt film could be contained on the absorber plate without excessive loss, determine over what flow range the film was stable without solar flux, and observe the behavior of the film as the flow rate was increased from laminar to turbulent regimes.

As discussed in the previous section, at low flow rates the film is unstable and, because of surface tension forces, tends to break up into discrete rivulets. Under no-flux conditions at 600 deg C, a minimum flow rate for a stable film should be 0.67 m^2/h, according to Hartley and Murgatroyd's model. Experimentally we found that at 611 deg C we could reduce the flow to 0.34 m^2/h before the film broke up into rivulets. Thus, it appears that their model is a conservative estimate of the minimum stable flow rate in the absence of flux.

We observed only smooth films over the entire flow rate range with the carbonate salt. It is well-known that such films, even in the laminar flow regime, quickly develop well-defined roll waves (17). Brauner and Maron (18) correlated the flow length required to develop the waves, normalized by the Nusselt film thickness, against the Reynolds number. Using the properties of our carbonate salt at 500 deg C, we find that at a Reynolds number (Γ/μ) = 250, 1.17 m is needed to develop the waves. Since this increases with Reynolds numbers, this explains why we never saw waves on our 0.61-m-long absorber. The existence of these waves greatly increases heat transfer (17), and we will see shortly that the absence of these waves affected our heat transfer results. Recently, we performed a flow visualization test with nitrate salts and were able to observe waves. This is also consistent with Brauner and Maron's correlation that predicts that this lower viscosity salt requires 0.22 m to develop waves at the same Reynolds number of 250.

Thermal Efficiency

The thermal efficiency of the salt film is defined as the energy delivered by the salt divided by the flux incident on the absorber. In terms of experimental data, this can be expressed by

$$\eta_t = \rho Q C_p [\bar{T}(x = L) - T_0] / \int_0^L q(x)\, dx \,, \qquad (5)$$

where $\bar{T}(x = L)$ is the bulk film temperature at the exit of the absorber. This definition of η_t circumvents details of the cavity design and allows us to state the efficiency of the film alone.

We noticed that a major contributor to experimental errors, especially in measuring the film efficiency, was unsteadiness, which is inherent in testing under actual solar conditions. As a result, we carefully screened efficiency data for steady conditions. These are presented in Fig. 5 along with results of the

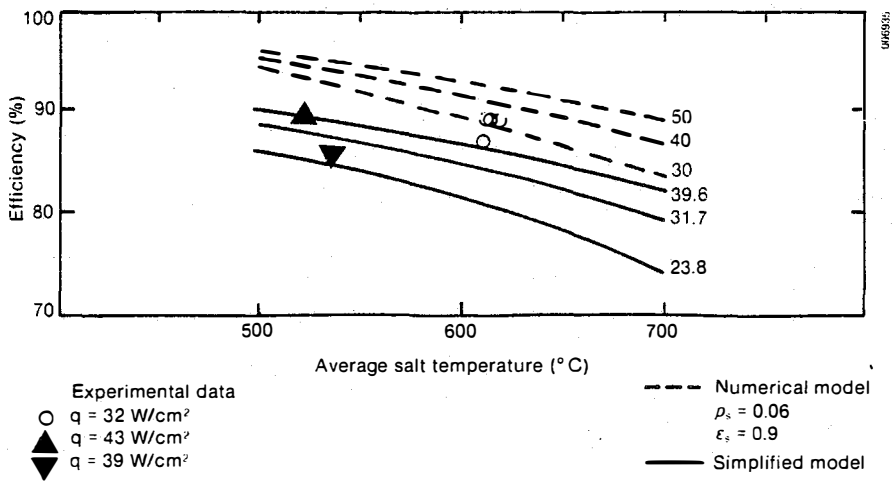

Fig. 5. DAR Film Thermal Efficiency

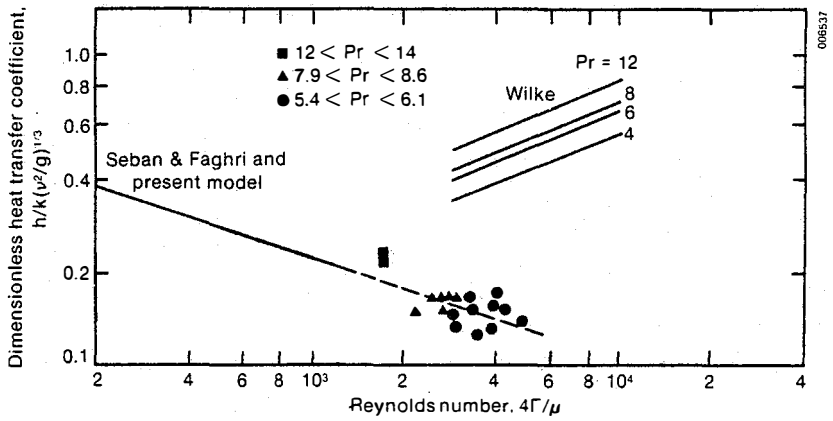

Fig. 6. Dimensionless Heat Transfer Coefficient

numerical model and the simplified model described previously. For the simplified model we used a reflectance of 0.06 per Jorgensen (19), and an emissivity for the salt film of 0.90. Data are presented with flux as a parameter, and one can see that the simplified model is more conservative than the numerical model, generally lying about 4% below the numerical model. The numerical model should agree with the simple model, but because the losses are quite small, numerical errors amplify the calculated losses. The experimental data at 500 deg C and 600 deg C agree quite favorably with the simple model, generally within about 4%, well within experimental uncertainties.

Using the simplified model [equation (4)] as a guide, the behavior seen in Fig. 6 can be explained. Losses from the film are essentially flux in the solar wavelengths reflected at the salt-air interface and reradiation from the film. The latter increases with increasing film temperature, thereby reducing efficiency. Increasing the flux at a fixed film temperature increases the efficiency according to equation (4) because the reradiation losses are relatively smaller.

Heat Transfer from the Absorber to the Film

Of primary concern here is the difference in temperature between the flowing salt film and the absorbing surface. This quantity is quite sensitive to the transmissivity of the salt film and the wavelength distribution of the flux because they determine how much energy is absorbed in the film versus how much is absorbed on the absorber surface and subsequently transferred to the salt.

We quantified this effect by plotting the dimensionless heat transfer coefficient $(h/k)(\nu^2/g)^{1/3}$ against the film Reynolds number, $4\Gamma/\mu$. Assuming a transparent film, the heat transfer coefficient is determined from the experimental data by

$$h(x) = \frac{(1 - \rho_s)q(x)}{T_s(x) - T_a(x)} . \qquad (6)$$

The local flux was measured as described previously. Local salt temperature was determined from

$$\frac{T_s(x) - T_{si}}{T_{so} - T_{si}} = W \int_{inlet}^{x} q(z)\, dz/Q_{in} . \qquad (7)$$

The local heat transfer coefficients were determined at five locations, x. To correlate the dimensionless heat transfer coefficient against Re and Pr, we determined property values at the mean salt temperature.

To calculate the average dimensionless heat transfer coefficient, we used the local heat transfer at the

most downstream absorber location, which was in the region of thermal equilibrium. Results for all runs, grouped by Prandtl number, and those of the model are shown in Fig. 6.

Also shown in Fig. 6 are data of Wilke (20) for several Prandtl numbers in the turbulent regime and two models for the laminar region. The first laminar model is by Seban and Faghri (12) for laminar films. Wilke's turbulent data are for falling water and water-ethylene glycol mixtures on the exterior of a vertical tube. The low end of Wilke's data depicts the departure from laminar flow based on his observations of the departure of the heat transfer data from laminar behavior. The second model is our numerical model that gives virtually identical results to the Seban and Faghri curve.

Although our experimental data are for Reynolds numbers well into the turbulent regime, they appear to closely follow an extrapolation of the laminar curves. This behavior is consistent with our visualization of the film as discussed previously. With the carbonate salt we always observed a smooth film. Presumably, measurements with the nitrate salt, where we have observed wavy behavior, would exhibit much higher heat transfer coefficients, which is more consistent with Wilke's data in Fig. 6.

Salt-Film Stability

As discussed previously, one of the important purposes of this test program was to determine if the salt film was stable over the range of flow rates anticipated for the DAR. (By stable we are referring to a condition in which the salt film uniformly wets the absorber panel.) The flow rate range of interest (per unit width) is from 14.9 m^2/h at the high end down to below 3.7 m^2/h. The upper range corresponds to a full power direct absorption receiver and the lower end of the range corresponds to a smaller receiver operating with a turn-down factor of 3. As discussed previously, we achieved stable flows in the absence of flux as low as 0.34 m^2/h on the absorber panel. We did not experience any salt film instability in the high-flow regime.

Experimentally, we found that flow rates below about 10.4 m^2/h with flux produced what appeared to be a local dry area on the plate and local overtemperatures. The dry area started near the top at the west edge and gradually widened to about 5 cm near the bottom of the absorber. Close observation of the dry area showed that it actually was a region of slightly reduced film thickness at 10.4 m^2/h that became thinner as the flow decreased. At 4.5 m^2/h the region had thinned sufficiently to become a dry patch.

This behavior was surprising because it occurred at a flow rate so much greater than the no-flux breakdown flow predicted by Hartley and Murgatroyd (15). We have not yet determined the mechanism for the formation of this dry area, but we have two hypotheses. First, we noticed that the raised edges used to contain the salt during no-flux tests (see Fig. 3) completely dried out during flux tests for flows below about 7.5 m^2/h and became very hot. Heat transfer from these edges could precipitate a thermocapillary flow and cause the dry area to form. Second, the model and data of Simon and Hsu (16) as discussed previously could describe a breakdown phenomenon like we saw. We are planning laboratory tests with an artificial flux source to test both of these hypotheses.

The flow rates at which we observed the dry area are not excessively high. A commercial DAR may well operate above these flow rates under nominal conditions. However, during part load and because of flux variations across the absorber panel, one must be aware of any minimum flow requirements.

CONCLUSIONS

The experiments provide the necessary data to further establish that the concept is feasible for use in solar thermal central receiver systems, although film behavior needs to be further assessed to attain increased confidence. The results of the experimental work can be highlighted as follows:

- The salt film is stable at flow rates high enough to be of commercial interest.
- Thermal efficiency of the salt film is in the range of 80%-90%, depending on salt film temperature and flux.
- Heat transfer coefficients between the absorber surface and the salt film should exceed 3000 W/m^2 deg C keeping the absorber no more than 150 deg C above the bulk-salt temperature for flux levels of about 500 suns, assuming no dopant was added to the salt to darken it. These heat transfer coefficients should approximately double for absorbers longer than 1.2 m for carbonate salt. Adding a dopant to the salt greatly reduces the absorber temperature for a given flux and salt-film temperature.
- The existing model, which predicts efficiency and heat transfer coefficients (or equivalently, absorber temperatures), can be used with confidence in the flow regime tested, assuming certain property values are determined with greater confidence in the future. The simplified model also predicts thermal efficiency reasonably well.

The experiments conducted at the ACTF were limited to a small-size absorber plate and to flux levels in the range of 15-60 W/cm^2. Because of these facility constraints, extrapolation of test results to other situations requires great care. For example, the following items are elaborated for the readers benefit: a change from the carbonate salt used in this study could alter some of the conclusions of this work; a possible stability problem exists for most flux levels with salt flows below 10.4 m^2/h; special care needs to be taken at absorber edges to prevent dryout and salt decomposition; operation above 50 W/cm^2 flux will most likely require that the salt be doped to enhance absorption in the solar spectrum; and certain property values for the molten carbonate salt, notably the solar- and infrared-weighted extinction coefficients and thermal conductivity, need to be determined before the model can reliably predict receiver performance.

ACKNOWLEDGMENT

We wish to acknowledge and express our gratitude to the Solar Thermal Technology Program of the Department of Energy that sponsored this research.

REFERENCES

1. Hruby, J. M. and Steele, B. R., "Design and Performance Evaluation of a Solid Particle Solar Central Receiver," presented at the AIChE Summer National Meeting, August 1985, Seattle, Paper No. 60E.

2. Hunt, A. J., "Small Particle Heat Exchangers," LBL-7471, 1978, Lawrence Berkeley Laboratory, Berkeley, Calif.

3. Bohn, M., et al., "Direct Absorption Receiver Experiments and Concept Feasibility," SERI/TR-252-2884, Nov. 1986, Solar Energy Research Institute, Golden, Colo.

4. Brumleve, T. D., "A High-Temperature Solar Energy System," SAND 74-8008, 1974, Sandia National Laboratories, Albuquerque, N. Mex.

5. Brumleve, T. D., "Status Report on the Direct Absorption Receiver," SAND 78-8702, 1978, Sandia National Laboratories, Albuquerque, N. Mex.

6. Wang, K. Y. and Copeland, R. J., "Heat Transfer in a Solar Radiation Absorbing Molten Salt Film Flowing over an Insulated Substrate," ASME paper 84-WA/Sol-22, 1984.

7. Webb, B. W. and Viskanta, R., "Analysis of Heat Transfer and Solar Radiation Absorption in an Irradiated Thin, Falling Molten Salt Film," Journal of Solar Energy Engineering, Vol. 107, No. 2, 1985, pp. 113-119.

8. Wang, K. Y., "Heat Transfer in a Molten Salt Film: An Application for Direct Absorption Receivers," forthcoming, Solar Energy Research Institute, Golden, Colo.

9. Newell, T. A., Wang, K. Y., and Copeland, R. J., "Falling Film Flow Characteristics of the Direct Absorption Receiver," SERI/TR-252-2641, Mar. 1986, Solar Energy Research Institute, Golden, Colo.

10. Maron, D. M., Brauner, N., and Dukler, A., "Interfacial Structure of Thin Falling Films: Piecewise Modelling of the Waves," PhysicoChemical Hydrodynamics, Vol. 6, 1985, pp. 87-113.

11. Seban, R. A., "Transport to Falling Films," 6th Int. Heat Transfer Conf., 1978, pp. 417-428.

12. Seban, R. A. and Faghri, A., "Evaporation and Heating with Turbulent Falling Films," Journal of Heat Transfer, Vol. 98, 1976, pp. 315-318.

13. Takahama, H. and Kato, S., "Longitudinal Flow Characteristics of Vertically Falling Films without Concurrent Gas Flow," Int. J. Multiphase Flow, Vol. 6, 1980, pp. 203-215.

14. Hirshburg, R. I. and Florschuetz, L. W., "Laminar Wave-Film Flow: Part I, Hydrodynamic Analysis," Journal of Heat Transfer, Vol. 104, 1982, pp. 452-458.

15. Hartley, D. E., and Murgatroyd, W. "Criteria for the Break-up of Thin Liquid Layers Flowing Isothermally Over Solid Surfaces," Int. J. Heat Mass Transfer, Vol. 7, 1964, pp. 1003-1015.

16. Simon, F. F. and Hsu, Y., "Thermocapillary Induced Breakdown of a Falling Liquid Film," NASA TN D-5624, 1970.

17. Dukler, A. E., "Characterization, Effects and Modeling of the Wavy Gas-Liquid Interface," Proceedings of the International Symposium on Two-Phase Systems, Vol. 6, 1972, pp. 207-234.

18. Brauner, N. and Maron, D. M., "Characteristics of Inclined Thin Films, Waviness and the Associated Mass Transfer," Int. J. Heat Mass Transfer, Vol. 25, 1982, pp. 99-110.

19. Jorgensen, G. J., Schissel, P., and Burrows, R. W. "Optical Properties of High-temperature Materials for Direct Absorption Receivers," presented at the 29th Annual International Technical Symposium on Optical and Electro-optical Engineering, Aug. 1985, San Diego, Calif.; also SERI/TP-255-2791, Solar Energy Research Institute, Golden, Colo.

20. Wilke, W., V.D.I. Forschungsheft, No. 490, 1962, Dusseldorf, Germany.